ACCOUNTS
of chemical research

Chemistry of Ni^{2+} in Urease: Sensing, Trafficking, and Catalysis

BARBARA ZAMBELLI,[†] FRANCESCO MUSIANI,[†]
STEFANO BENINI,[‡] AND STEFANO CIURLI[*,†,§]

[†]*Laboratory of Bioinorganic Chemistry, University of Bologna, Italy,* [‡]*Faculty of Science and Technology, Free University of Bolzano, Italy, and* [§]*CERM (Center of Magnetic Resonance), University of Florence, Italy*

RECEIVED ON FEBRUARY 18, 2011

CONSPECTUS

Transition metals are both essential to enzymatic catalysis and limited in environmental availability. These two biological facts have together driven organisms to evolve mechanisms for selective metal ion sensing and utilization. Changes in metal ion concentrations are perceived by metal-dependent transcription factors and transduced into appropriate cellular responses, which regulate the machineries of competitive metal ion homeostasis and metalloenzyme activation. The intrinsic toxicity of the majority of metal ions further creates a need for regulated intracellular trafficking, which is carried out by specific chaperones.

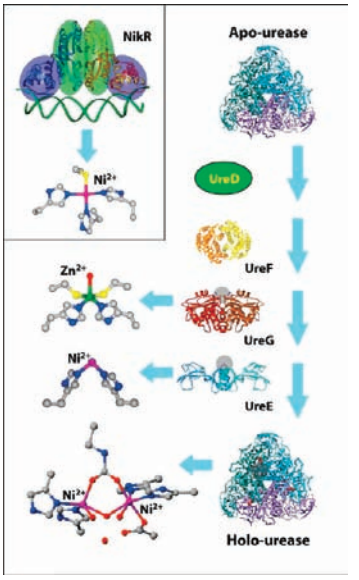

The Ni^{2+}-dependent urease enzymatic system serves as a paradigm for studying the strategies that cells use to handle an essential, yet toxic, metal ion. Although the discovery of urease as the first biological system for which nickel is essential for activity dates to 1975, the rationale for Ni^{2+} selection, as well as the cascade of events involving metal-dependent gene regulation and protein–protein interactions leading to enzyme activation, have yet to be fully unraveled. The past 14 years since the Account by Hausinger and co-workers (Karplus, P. A.; Pearson, M. A.; Hausinger, R. P. *Acc. Chem. Res.* 1997, *30*, 330–337) have witnessed impressive achievements in the understanding of the biological chemistry of Ni^{2+} in the urease system. In our Account, we discuss more recent advances in the comprehension of the specific role of Ni^{2+} in the catalysis and the interplay between Ni^{2+} and other metal ions, such as Zn^{2+} and Fe^{2+}, in the metal-dependent enzyme activity. Our discussion focuses on work carried out in our laboratory.

In particular, the structural features of the enzyme bound to inhibitors, substrate analogues, and transition state or intermediate analogues have shed light on the catalytic mechanism. Structural and functional information has been correlated to understand the Ni^{2+} sensing effected by NikR, a nickel-dependent transcription factor. The urease activation process, involving insertion of Ni^{2+} into the urease active site, has been in part dissected and analyzed through the investigation of the molecular properties of the accessory proteins UreD, UreF, and UreG. The intracellular trafficking of Ni^{2+} has been rationalized through a deeper understanding of the structural and metal-binding properties of the metallo-chaperone UreE. All the while, a number of key general concepts have been revealed and developed. These include an understanding of (i) the overall ancillary role of Zn^{2+} in nickel metabolism, (ii) the intrinsically disordered nature of the GTPase responsible for coupling the energy consumption to the carbon dioxide requirement for the urease activation process, and (iii) the role of the accessory proteins regulating this GTPase activity.

Role of Nickel for the Enzymatic Activity of Urease

Urease catalyzes urea hydrolysis in the last step of organic nitrogen mineralization to give ammonia and carbamate, which decomposes to give a second molecule of ammonia and bicarbonate (Scheme 1). The hydrolysis of the reaction products induces an overall pH increase that has negative implications both in human and animal health as well as in the ecosphere.

Published on the Web 05/04/2011 www.pubs.acs.org/accounts
10.1021/ar200041k

The structures of urease from the bacteria *Klebsiella aerogenes* (KAU),[1] *Bacillus pasteurii* (BPU),[2] and *Helicobacter pylori* (HPU),[3] and from the seeds of the plant *Canavalia ensiformis* (jack bean, JBU)[4] have revealed the molecular architecture of this enzyme. The quaternary structure of the majority of bacterial ureases, including KAU and BPU, is composed of a trimer of trimers $(\alpha\beta\gamma)_3$, with each α subunit containing an active site (Figure 1A,B).[1,2] In HPU, four trimers of dimers $(\alpha\beta)_3$ (with the β subunit resulting from the fusion of the corresponding β and γ subunits found in BPU and KAU) form a tetrahedral structure $((\alpha\beta)_3)_4$ with a total of twelve active sites per HPU functional molecule (Figure 1C).[3] The plant enzyme consists of a dimer of homotrimers $(\alpha_3)_2$, evolved from the fusion of the corresponding bacterial $\alpha\beta\gamma$ trimer, and contains six active sites (Figure 1D).[4]

Urea decomposes into cyanic acid and ammonia with a half-life of 33 years through an ammonia elimination mechanism, while the half-life for spontaneous hydrolysis to yield ammonia and carbamate is 520 years.[5] In the case of urease, the half-life for the catalytic hydrolysis is 20 ms: this results in a rate enhancement of 3×10^{15}, much higher than that of all other known hydrolases.[5]

The urease active site (Figure 2A) contains two Ni^{2+} separated by 3.5−3.7 Å, bridged by the oxygen atoms of a carbamylated lysine residue, and bound to two histidines. One Ni^{2+} ion is additionally bound to an aspartate carboxylate oxygen. The coordination geometry of the Ni^{2+} ions is completed by a water molecule terminally bound to each metal ion and by a nickel-bridging hydroxide ion. This ligand arrangement yields one penta-coordinated Ni^{2+} ion with a distorted square-pyramidal geometry, and one Ni^{2+} ion hexa-coordinated with a distorted octahedral geometry. An additional water molecule is part of a hydrogen-bonding network completing a tetrahedral cluster of four water/hydroxide molecules in the close proximity of the Ni^{2+} ions, hinting to the existence of an active site cavity prebuilt to stabilize a tetrahedral transition state and/or intermediate. A mobile flap modulates the entrance of the substrate to the active site cavity, with a catalytically essential histidine moving by about 5 Å between the open (Figure 2B) and closed (Figure 2C) conformations.

SCHEME 1

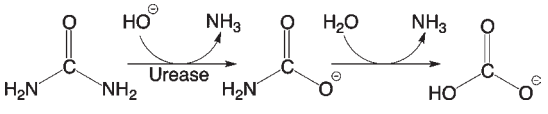

The structure of BPU, in the native hydrated form and complexed with several inhibitors of different chemical classes, suggests a structure-based reaction mechanism for urease (Scheme 2).[6] The mechanism entails a hydrated state of the enzyme (Scheme 2A) that, upon entrance of urea when the flap is open, evolves to give an initial substrate-bound intermediate (Scheme 2B). Urea binds to $Ni_{(1)}$ using the carbonyl oxygen and displaces the water molecules. This step is corroborated by docking and density-functional quantum chemistry calculations,[7] which also suggest that flap closure facilitates urea coordination to the second Ni^{2+} via its $-NH_2$ group, stabilized by a specific H-bonding network (Scheme 2C). The viability of this bidentate urea coordination mode is supported by the crystal structure of BPU in complex with $B(OH)_3$, featuring the hydroxyl groups of $B(OH)_3$ replacing the water molecules.[8] Boric acid is isoelectronic with urea, has the same neutral charge, triangular shape, and dimension, and can be considered an inert analogue of the substrate. In this binding situation, the carbon atom of urea undergoes the nucleophilic attack by the Ni^{2+}-bridging hydroxide, whose bonds with the metal ions have been weakened by the binding of the substrate, leading to the tetrahedral intermediate (Scheme 2D). This step, supported by calculations,[7] is corroborated by the structure of BPU crystallized in complex with phenylphosphorodiamidate (PPD), where the product of the hydrolysis of PPD, diamidophosphate (DAP), had been trapped in the active site replacing the cluster of four water/hydroxide molecules.[2] DAP is an analogue of the tetrahedral transition state or intermediate of the enzymatic reaction.

The nickel-bridging $-OH$ group, now part of a diamino(hydroxy)methanolate moiety and therefore very acidic, can transfer the hydrogen atom to the distal urea NH_2 group. This event could occur via the nearby oxygen atom of the $Ni_{(2)}$-bound aspartate, which is able to undergo a dihedral rotation along the $C\alpha-C\beta$ bond, approaching alternatively the bridging hydroxide or the distal $-NH_2$ group.

The neutral imidazole side chain of the active site conserved histidine residue, moving nearer the active site upon closure of the flap, stabilizes the nascent $C-NH_3^+$ group (Scheme 2E). The distal C−N bond is broken, ammonia is released, and the resulting carbamate decomposes into NH_4^+ and bicarbonate. The flap opening could facilitate the release of products and allow bulk water to rehydrate the active site to yield the native state of the enzyme (Scheme 2A). These steps could occur in a concerted manner. This mechanism is in agreement with all kinetics data, in particular the pH-dependence of the enzyme activity and the

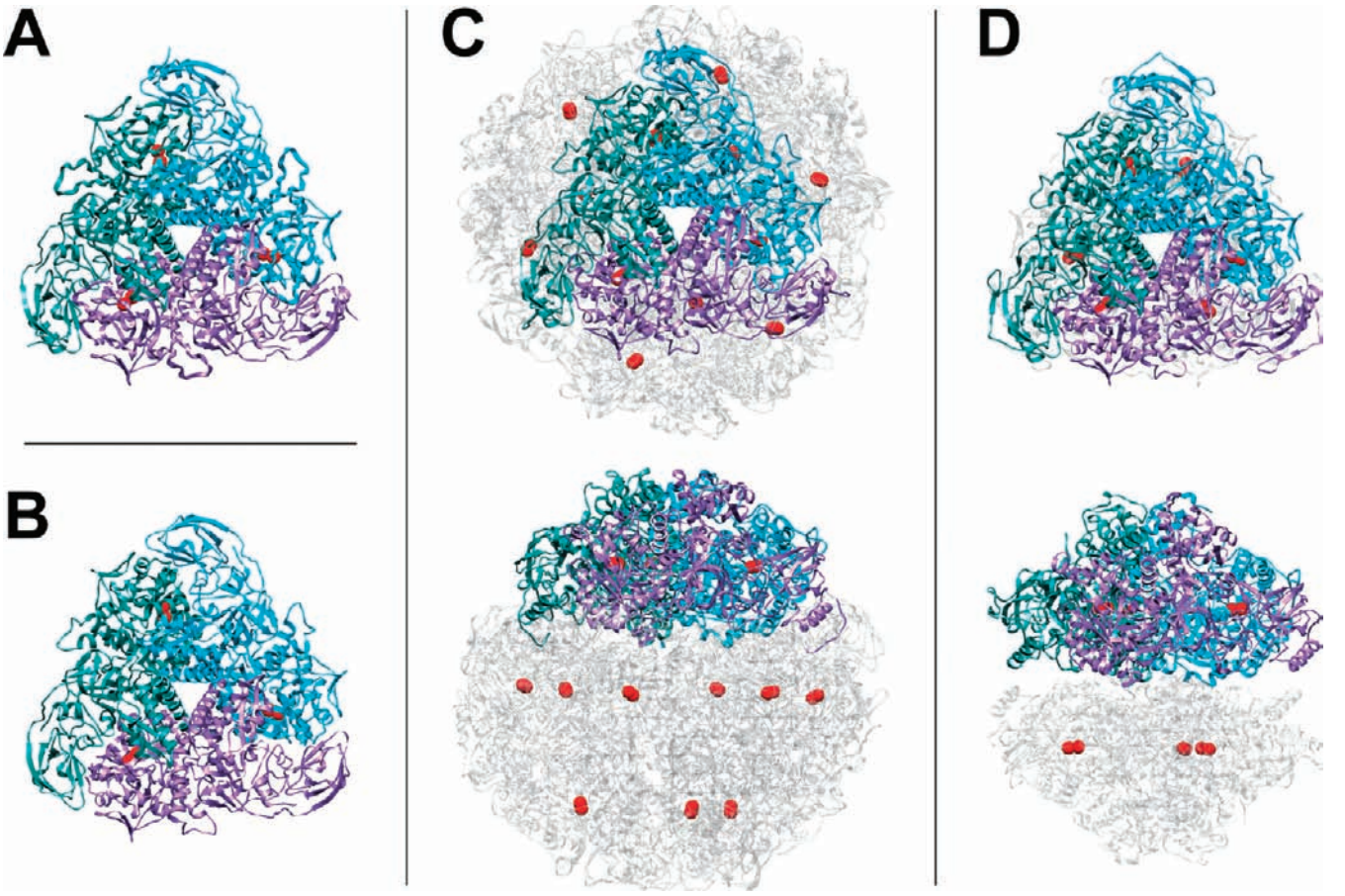

FIGURE 1. Ribbon diagram of urease from (A) *B. pasteurii* (PDB code: 2UBP), (B) *K. aerogenes* (PDB code: 1EJZ), (C) *H. pylori* (PDB code: 1E9Z), and (D) jack bean (PDB code: 3LA4). Ribbon colors evidence the chains composing the trimer of oligomers (monomers in the case of jack bean) constituting the minimal quaternary structure of urease. Ni^{2+} are reported as red spheres. The bottom panels of (C) and (D) are rotated by 90° around the horizontal axis vs the top panels.

noncompetitive inhibition by fluoride, thought to replace the bridging hydroxide.

The presence of catalytic Ni^{2+} in urease has puzzled scientists since its first observation.[9] The less toxic d^{10} closed-shell Zn^{2+} is usually observed in hydrolytic enzymes, because of its large positive charge density and its resilience to undergo deleterious redox state changes. However, these properties are also applicable to Ni^{2+}, which additionally features an open-shell d^8 electronic configuration that induces stereoelectronic requirements. This property could be exploited by Ni^{2+} to drive the two substrates, urea and water, into the optimal spatial topology necessary for catalysis, as shown in all steps of the mechanism where the two Ni^{2+} are either penta-coordinated in a distorted square-pyramid for $Ni_{(1)}$, or hexa-coordinated in a distorted octahedron for $Ni_{(2)}$. These geometries are commonly observed for nickel but not for zinc, which is usually tetra-coordinated in enzyme catalytic sites. Given the ligand arrangement observed in the active site of urease, a Zn^{2+} ion in place of $Ni_{(1)}$ would be four-coordinated and unable to bind a molecule of urea. Similarly, a Zn^{2+} ion in place of $Ni_{(2)}$ would be five-coordinated and therefore unable to additionally bind the urea $-NH_2$ group in the step that leads to the bidentate substrate binding mode.

An exception to the strict requirement of urease for Ni^{2+} is represented by urease from *H. mustelae*, a bacterium that colonizes the stomach mucosa of carnivore animals. The genome of this bacterium codifies for two urease enzymes: one is a typical nickel-dependent urease, while the other one is characterized by the absence of Ni^{2+}, by inactivation in the presence of oxygen, and by Fe^{2+}-induced expression.[10] These observations suggest that the alternative urease contains Fe^{2+} in its active site. This metal ion is sensitive to oxidation but features the same charge, similar radius and stereoelectronic propensity as Ni^{2+}, thus adhering to the rationale described above for its suitability to act as a cofactor in this enzyme.

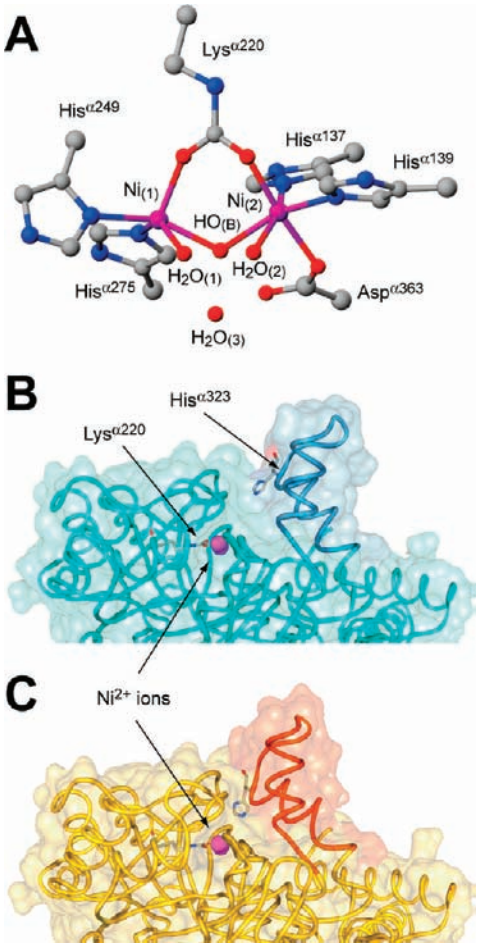

FIGURE 2. Coordination geometry of Ni^{2+} in native urease active site (A, 2UBP). Color scheme: nickel, purple; carbon, gray; nitrogen, blue; oxygen, red. Open (B, 2UBP) and closed (C, 3UBP) conformation of the flexible flap. Ni^{2+} are shown as purple spheres.

Nickel-Dependent Transcriptional Regulation of Urease Genes

The essentiality of Ni^{2+} for urease activity, together with the environmental scarcity of this metal ion, led urease-dependent organisms to evolve mechanisms that correlate intracellular Ni^{2+} availability with urease gene activation.[11] In particular, in *Helicobacter pylori*, the expression of the urease operon is regulated by the Ni^{2+}-dependent sensor NikR. This homotetrameric protein belongs to the class of ribbon−helix−helix (RHH) transcription factors, as revealed by the crystal structures of the protein from *E. coli* (*Ec*), *Pyrococcus horikoshii* (*Ph*), and *H. pylori*.[12] NikR is made of two dimeric N-terminal DNA-binding domains (DBD), containing RHH motifs, extending at the sides of an inner C-terminal domain, responsible for tetramerization and metal binding (metal binding domain, MBD). The DBD and MBD are connected by a linker, whose flexibility allows NikR to adopt different protein conformations ("open", "trans", and "cis") depending on the relative orientation of the DBD with respect to the MBD (Figure 3). In the DNA-bound form, the DBD are locked in the "cis" configuration, with the RHH motifs in contact with two operator half-sites spaced by two turns of the DNA helix (Figure 3C).

NikR binds four low-spin d^8 Ni^{2+} in a square-planar coordination geometry comprising conserved, canonic, His_3Cys sites at the protein tetramerization interface (Figure 4).[12] In *Hp*NikR, these four metal-binding sites are organized in two sets, with a 2 + 2 stoichiometry and binding affinities differing by one order of magnitude.[13] This observation is consistent with their topological structural organization, arranged in two pairs of more closely (ca. 15 Å) and two pairs of more distantly (ca. 22 Å) spaced metal ions. The overall affinity of these sites for Ni^{2+} increases at higher pH, consistently with a proton dissociation event involving the cysteine residue.[13] The two pairs of binding sites feature different dependence on pH, with the first set being almost pH-independent, and the second set decreasing its affinity by one order of magnitude in the pH range 6.5−8.0.[13] The crystal structures of Ni^{2+}-bound *Hp*NikR, obtained at non-physiologically low pH (pH range 4.6−5.6), exhibited two, and not four, canonic sites occupied by square-planar Ni^{2+} ions together with additional octahedral binding sites possibly generated by the acidic crystallization conditions.[14,15]

*Hp*NikR can bind different metal ions beside Ni^{2+} in vitro, such as Zn^{2+}, Co^{2+}, and Cu^{2+}.[16] However, the protein response to metal binding is Ni^{2+}-selective in vivo. The preference of Ni^{2+} over Co^{2+} and Cu^{2+} can be explained by considering the 10-fold lower affinity of Co^{2+}[16] or the low availability of Cu^{2+} in the intracellular reducing environment. Differently, Zn^{2+} binds *Hp*NikR with affinity comparable to that of Ni^{2+},[16] and its intracellular concentration is orders of magnitude higher than that of Ni^{2+}.[17] This metal-bound promiscuity is coupled with metal-selectivity of *Hp*NikR through a close connection between malleable protein backbone and rigid metal ion coordination geometry.[16] Ni^{2+} binding to the first pair of sites imposes the square planar coordination geometry preferred by the d^8 configuration, driving the correct configuration of the second pair of sites. Differently, Zn^{2+} (d^{10}) can bind the first pair of sites, but its lack of stereoelectronic constraints renders it unable to force the protein into a situation favorable to the correct filling of the second pair of sites, leading to an aberrant 2 + 4 metal binding stoichiometry.[16] This observation is supported by structural data obtained on the MBD of *Ec*NikR bound to Zn^{2+}.[12] Subsequent to Ni^{2+} binding, the flexibility of the protein matrix appears to propagate this chemical

SCHEME 2

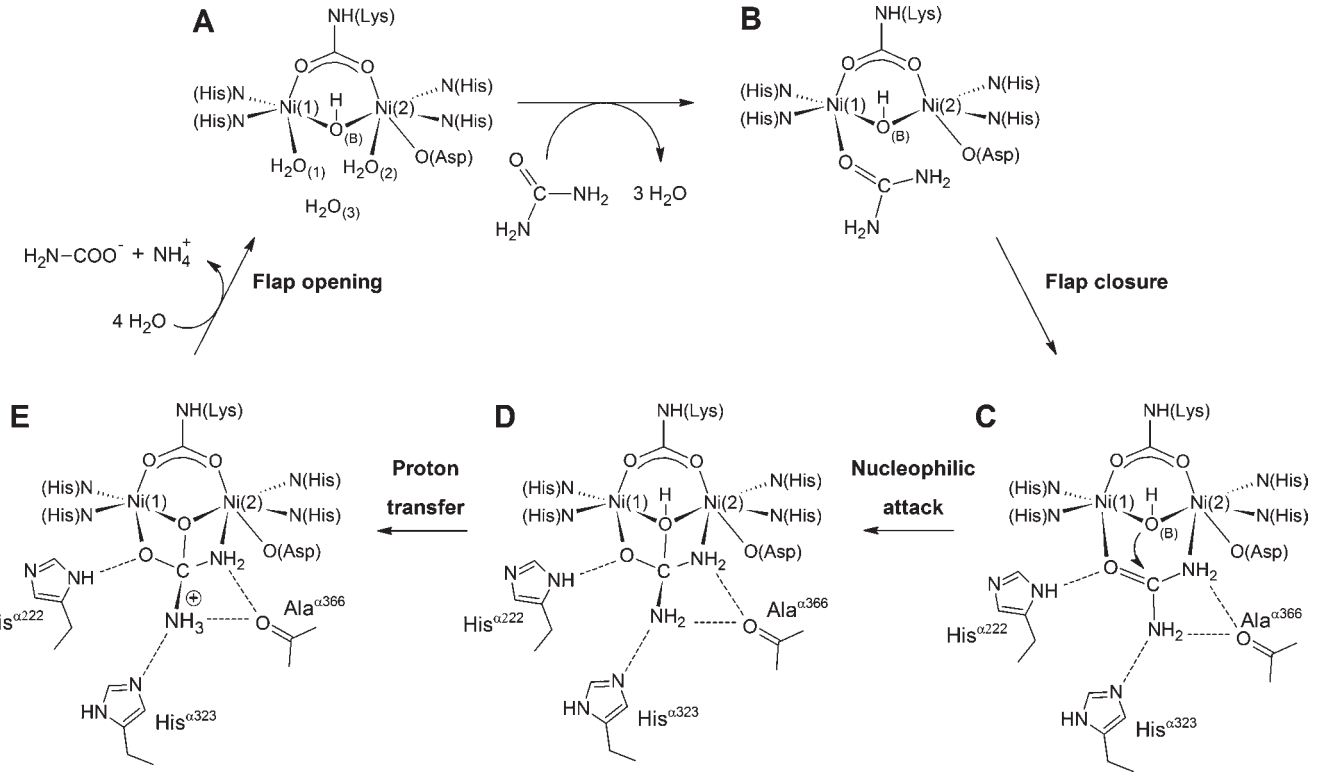

information away from the MBD to the DBD. Accordingly, a slow conformational change ($k < 5 \times 10^{-3}$ s^{-1}), induced by Ni^{2+} and not by Zn^{2+}, was observed.[16] The nature of the structural change needed to obtain a DNA-binding conformation of *Hp*NikR is an increment of flexibility in the linker connecting the DBD and MBD, which unlocks the position of the DBD with respect to the protein core.[18]

Nickel Trafficking toward Urease Activation

In vivo, apo-urease undergoes an activation process involving events such as CO_2 uptake for lysine carbamylation, hydrolysis of GTP, and Ni^{2+} delivery into its active site. These events, as well as the selectivity of the active site for Ni^{2+}, are regulated by cellular processes acting at the post-translational level and typically carried out by four dedicated accessory proteins: UreD, UreF, UreG, and UreE.

The need for both structural and accessory functions to attain a fully active enzyme is reflected by the presence of two groups of urease genes: three of them encode the apo-urease structural subunits (structural genes: *ureA*, *ureB*, *ureC*), while an additional four genes codify urease chaperones responsible for the assembly of the catalytic site (accessory genes: *ureD*, *ureF*, *ureG*, *ureE*). From a database search, we have identified 284 microorganisms (279 Bacteria and 5 Archea) for which the genome has been fully sequenced and that contain all urease structural genes (Figure 5). For the large majority of these genomes, structural and accessory proteins are codified by genes clustered in one or more operons, suggesting that their transcription is concomitantly regulated. Some genomes, such as the one of *H. mustelae* that additionally produces an Fe^{2+}-urease, contain more than one urease cluster. All complete urease operons could be classified in seven groups, according to the order adopted by urease genes on DNA (Figure 5 and Supporting Information Table 1SI). In particular, 70 operons (class 1), representing the most part of Gram-positive bacteria and some *Proteobacteria*, present structural genes (*ureA*, *ureB*, *ureC*) lying contiguously on DNA, and followed by the urease accessory genes (*ureE*, *ureF*, *ureG*, *ureD*) placed either in a flanking part or in a separate region of the chromosome. An additional 122 operons (class 2), representing the majority of *Proteobacteria* and *Cyanobacteria*, have *ureD* placed before *ureA*. The final five classes of operons show atypical orders of urease structural and accessory genes.

A full set of urease accessory genes is found in 213 (75%) of the identified ureolytic organisms. Among the organisms

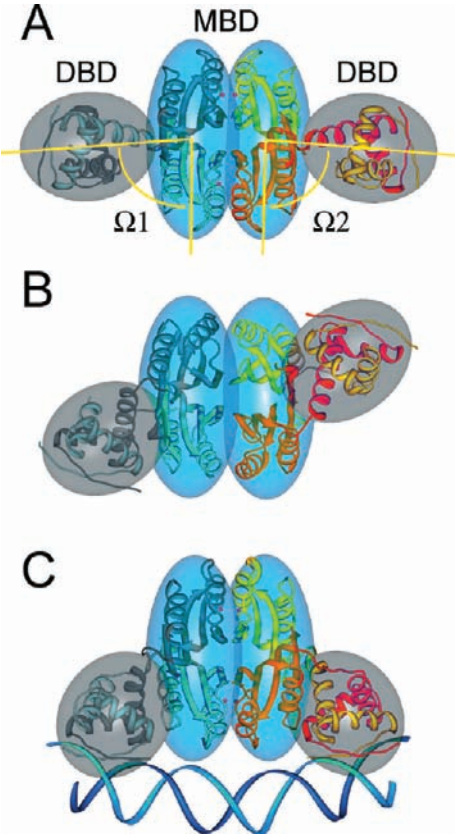

FIGURE 3. Ribbon diagrams and inertia ellipsoids of NikR in (A) open, (B) trans, and (C) cis conformation (PDB: 2HZA, 2CA9, and 2HZV, respectively).

lacking one or more of these genes, some express additional nickel-dependent enzymes, whose chaperones could substitute the missing urease chaperone functions (Supporting Information Table 2SI). The less conserved urease gene is *ureE*, which is absent in 37 organisms. Thirteen genomes lack *ureD*, five do not contain *ureG*, and only one does not have *ureF*. Six additional organisms lack both *ureE* and *ureF*, and another one lacks both *ureF* and *ureD*. Four genomes lack the set of *ureF*, *ureG*, and *ureD*, while in only four cases no known accessory protein is found. Among these, *B. subtilis* is able to activate urease independently of the presence of accessory chaperones.[19]

Ni^{2+} insertion into the urease active site requires an interaction network comprising the enzyme itself and its accessory proteins. The generally accepted process (Figure 6) derives from genetic studies of the *K. aerogenes* system: UreD, UreF, and UreG act together as a molecular chaperone driving a protein conformational change, lysine carbamylation, and GTP hydrolysis, while UreE behaves as the metallochaperone of the system.[20]

UreD. Little is known on the functional and structural properties of UreD, apparently the first protein that binds

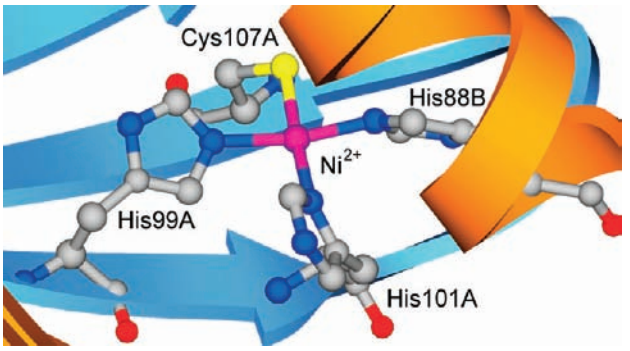

FIGURE 4. Structure of the metal binding sites found in *Hp*NikR (2Y3Y). Color scheme: nickel, purple; carbon, gray; nitrogen, blue; oxygen, red; sulfur, yellow.

apo-urease. The lack of information on this protein derives by its large insolubility when isolated in native conditions. A translational fusion of *Ka*UreD and maltose binding protein (MBP-UreD) has been purified and shown to bind Ni^{2+} and Zn^{2+} ions.[21] However, the physiological relevance of this chimerical product is uncertain, as UreD maintains its insolubility when separated from MBP. Moreover, MBP-UreD forms large multimers in solution (>670 kDa) that can partially complement the urease activation network. These observations suggest that MBP-UreD is present as an agglomeration of misfolded protein, maintained in solution by the folded and soluble MBP moieties.

UreF. This protein binds the urease-UreD complex, apparently through a direct interaction with UreD.[22] UreF was initially proposed to induce a conformational change to increase the active site accessibility for CO_2, and preventing incorrect Ni^{2+} binding to the noncarbamylated active site.[20] This hypothesis, however, would not explain why, in the presence of UreF, other divalent metal ions, such as Zn^{2+}, Co^{2+}, and Cu^{2+}, are not similarly excluded from the active site. On the basis of a protein structural model of *Bp*UreF, obtained by fold recognition analysis, this protein was suggested to contribute to the process of GTP hydrolysis as a GTPase activating protein (GAP).[23] This hypothesis appeared to reconcile all the previous functional data and could explain why the presence of UreF bound to the urease complex is necessary for UreG, the GTPase of the system, to join the activation complex.[24]

For several years, structural studies on UreF were prevented by its insolubility. The crystal structure of a truncated version of *Hp*UreF, lacking this C-terminal region (Figure 7A), reveals that *Hp*UreF is a homodimer, characterized by an all-helix fold that bears some similarity with GAP domains.[25] The structure appears to have little

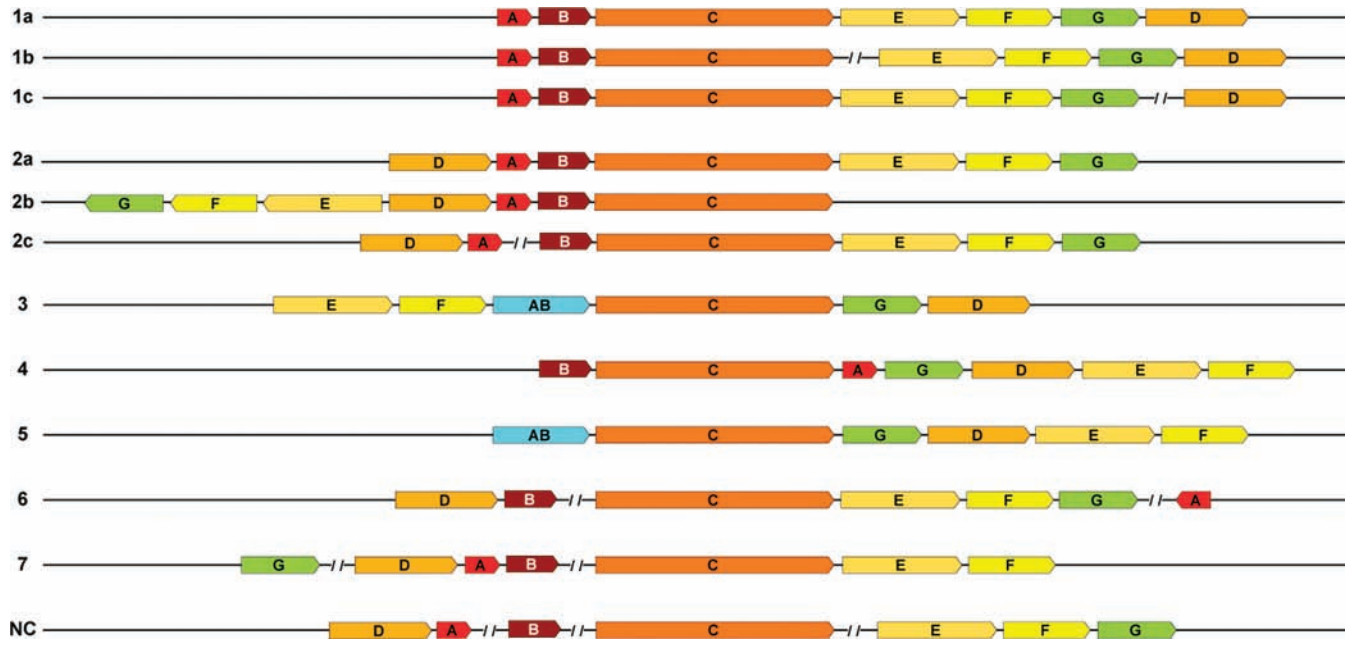

FIGURE 5. Schematic representation of urease operons in fully sequenced genomes (see Supporting Information Table 1). Arrows indicate the direction of the gene; the "//" symbol represents the presence of one or more non-urease genes between the evidenced urease genes. Arrow lengths are proportional to protein lengths. Classes are divided according to gene clustering order: 1a, ABCEFGD (54 organisms); 1b, ABC//EFGD (13 organisms); 1c, ABCEFGD differently clustered (3 organisms); 2a, DABCEFG (50 organisms); 2b, GFEDABC (16 organisms); 2c, DABCEFG differently clustered (57 organisms); 3, EFABCGD (10 organisms); 4, BCAGDEF (3 organisms); 5, ABCGDEF (1 organism); 6, DB//CEFG//A (1 organism); 7, G//DAB//CEF (1 organism); and NC, organisms with the complete set of urease genes not organized in a recognizable operon (24 organisms).

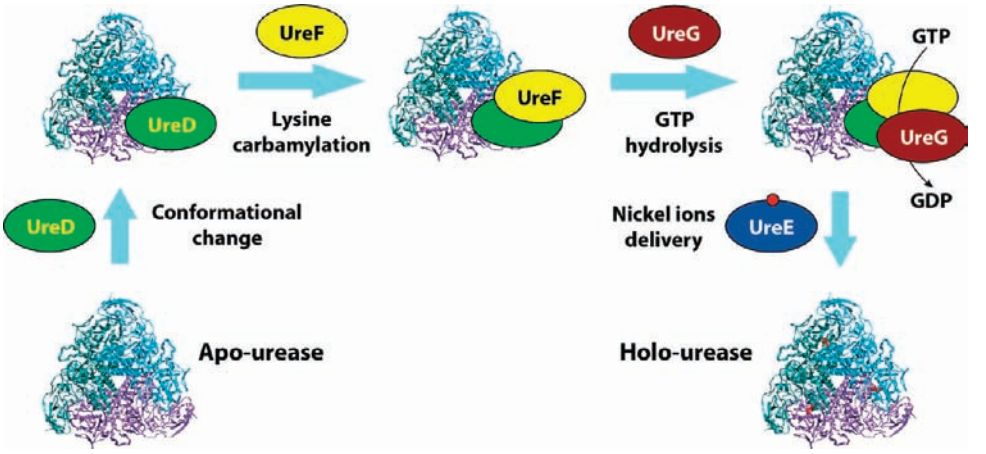

FIGURE 6. Proposed process for urease activation.

structural resemblance to known GTPase-activating proteins, even though a weak but intriguing structural similarity with several GAP domains of different origin was detected by homology searches,[25] thus not entirely excluding the hypothesis that UreF acts as a GAP involved in the GTPase cycle of UreG.

UreG. UreG is responsible for coupling GTP hydrolysis to the process of urease activation, and it is proposed to catalyze, in the presence of CO_2, the formation of carboxyphosphate, an excellent carbamylation agent for the metal-binding lysine in the urease active site.[24] The GTPase function is encoded in the protein sequence, which features a conserved N-terminal P-loop motif.

UreG proteins have been isolated and characterized from *K. aerogenes*,[26] *B. pasteurii*,[27] *M. tuberculosis*,[28] and *H. pylori*.[29] The solution properties of UreG are typical of proteins experiencing conformational equilibria, existing in solution as structural ensembles characterized by the presence of some secondary structure but lacking a well-defined tertiary structure.[27−30] This fluxional behavior, defined as "collapsed

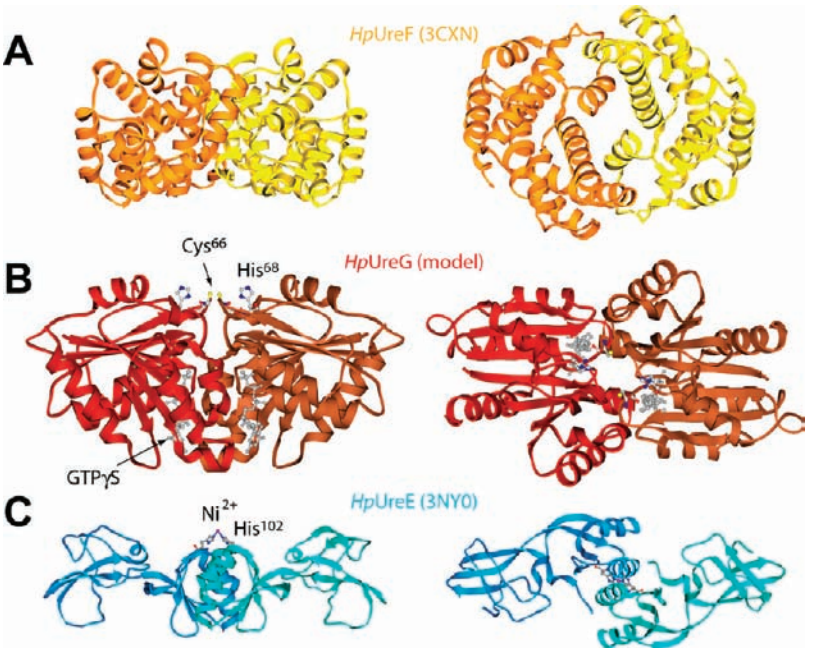

FIGURE 7. Ribbons diagram of *Hp*UreF (A, PDB code: 3CXN), *Hp*UreG model structure (B), and *Hp*UreE (C, PDB code: 3NY0). The positions of residues binding or proposed to bind metal ions and the position of GTPγ*S* in *Hp*UreG and Ni^{2+} ions in *Hp*UreE are evidenced.

disorder" with the protein in a molten globule-like or pre-molten globule-like fold, inscribes UreG into the ever-growing class of intrinsically disordered proteins. The presence of intrinsic disorder in an enzyme is unusual and striking. Indeed, enzymes are considered as proteins that interact with substrates using a lock-and-key or induced-fit mechanism and a well-determined tertiary structure. Therefore, UreG is the first, and so far only, naturally occurring enzyme ever discovered with an intrinsically disordered tract.

The presence of various degrees of protein flexibility in different members of this protein family suggests that a disorder-to-order transition is a possible mechanism for UreG functioning in vivo, and that the functional activation of UreG occurs when the protein interacts with other protein partners, perhaps other urease chaperones, that trigger its active ordered form. Generally, GTP hydrolysis is regulated at different levels by the cells to avoid unnecessary consumption of GTP. A protein interaction network, involving different effectors such as GTPase activating proteins (GAP) and/or guanine nucleotide exchange proteins (GEP), is very common among GTPases. A possible GAP for UreG has been identified in UreF.[23] These observations suggest that native disorder may be another general mechanism that cells use to regulate enzymatic activity, allowing this protein, partially or totally inactive in the isolated state, to interact and be regulated by different protein partners. The structures of the hypothetical folded state of several UreG proteins have been calculated (Figure 7B), and these models are in full agreement with all available chemical and biochemical data.[29]

According to sequence analysis, UreG belongs to the class of SIMIBI GTPases and ATPases, functioning as homo- or heterodimers in solution. In this dimeric form, interaction with one or more, dimeric, protein partners occurs and regulates GTPase activity. *Bp*UreG and *Mt*UreG are dimers in native conditions, while *Ka*UreG and *Hp*UreG are monomeric proteins.[29] Metal ions can have a role in the modulation of UreG activity through control of the oligomerization state. Zn^{2+}-driven protein dimerization occurs in vitro for *Hp*UreG, with one Zn^{2+} ion binding at the protein dimerization interface using a conserved cysteine and histidine from each monomer.[29] The Zn^{2+} binding residues are essential for the ability of *Ka*UreG to activate urease in vivo,[31] suggesting that Zn^{2+} binding plays a physiological role for UreG in the urease maturation pathway, driving the assembly of a functional protein complex that includes the dimeric UreG. In the case of *Hp*UreG, Ni^{2+} binding, occurring with an affinity one order of magnitude lower as compared to Zn^{2+}, does not induce oligomeric changes, indicating that UreG can discriminate between different metal cofactors in the intracellular metal ion pool.[29]

UreE. The presence of UreE in the urease maturation complex facilitates urease activation,[20] suggesting that UreE is the metallo-chaperone in charge of delivering Ni^{2+}. The crystal structure of *Bp*UreE, of a truncated version of *Ka*UreE (H144**Ka*UreE) and of *Hp*UreE reveal a symmetric homodimer,

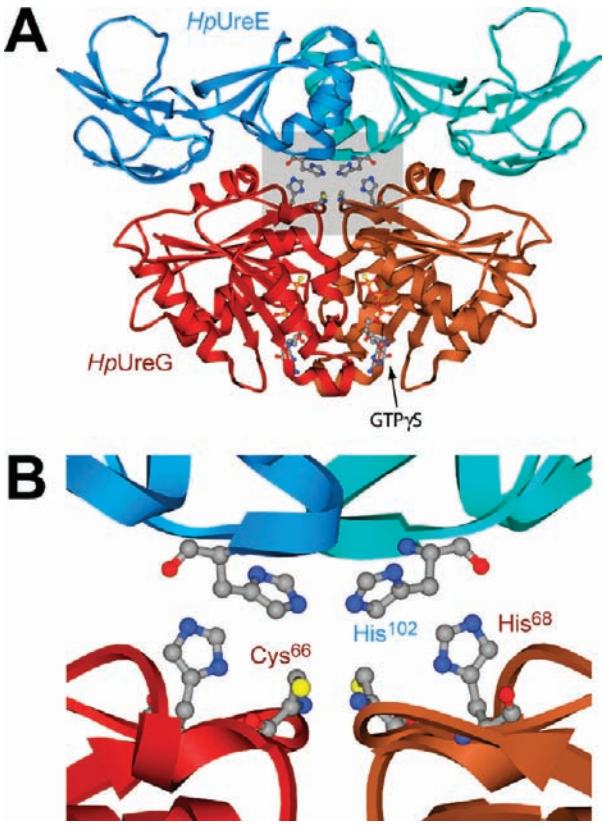

FIGURE 8. Ribbon diagram (A) and detail of the residues found at the interface of the complex and involved in metal binding (*Hp*UreE His^{102} and *Hp*UreG Cys^{66} and His^{68}) (B) of the model structure of the *Hp*UreE-*Hp*UreG complex (*Hp*UreE, blue and light blue; *Hp*UreG, red and brown-red).

with each monomers made of a C-terminal dimerization domain connected through flexible linkers to a peripheral N-terminal (Figure 7C).[32] A metal ion binding site is found at the protein dimerization interface, involving one conserved histidine from each monomer. *Bp*UreE and *Hp*UreE were crystallized as dimer of dimers in the presence of metal ions, with a single metal ion coordinated by the four conserved histidines at the protein tetramerization interface. This oligomeric form was found only in the solid state, or at very high concentrations (mM), and does not have any apparent physiological relevance.[33−35]

In some organisms, UreE contains a C-terminal His-rich tail able to provide additional Ni^{2+} binding capability. This sequence diversity is reflected in different metal binding properties of UreE from various sources. Equilibrium dialysis and ITC experiments on *Bp*UreE, *Ka*UreE, and its truncated form H144**Ka*UreE, which lacks the histidine-rich C-terminal sequence, revealed that these proteins bind two Ni^{2+} (*Bp*UreE and H144**Ka*UreE) or 5−6 Ni^{2+} (*Ka*UreE) per protein dimer with micromolar dissociation constants.[33,36] Similar experiments indicated that *Hp*UreE binds only one Ni^{2+} ion per protein dimer in the same position.[34,37] A reason for this diversity, besides the presence of absence of the natural His-rich tail, might reside in the number of histidines found at the protein C-terminus: while all UreE proteins contain at least one histidine residue in this region, suggesting its possible functional role,[32] both *Bp*UreE and *Ka*UreE contain at least one HXH motif, which in *Bp*UreE was proposed to be involved in the binding of a binuclear $[Ni(OH)Ni]^{3+}$ center.[33] On the other hand, *Hp*UreE contains a single histidine in this region, explaining the different stoichiometry of the Ni^{2+} binding to *Hp*UreE (1:1) and to *Bp*UreE and *Ka*UreE (2:1).

Among the different metal ions that UreE proteins can bind in vitro (Ni^{2+}, Zn^{2+}, Cu^{2+}, Co^{2+}), Zn^{2+} appears to have a physiological role in regulating the intracellular metal trafficking that leads to active site assembly in different Ni^{2+}-dependent enzymes: in particular, Zn^{2+} appears to have a role in the urease maturation process, through the dimerization of UreG.[29] Zn^{2+} and Ni^{2+} share the same binding site at the interface of the protein dimer in the *Bp*UreE crystal structure.[38] In *Ka*UreE, the affinity for Zn^{2+} is 10 times lower than the affinity for Ni^{2+},[36] while the thermodynamics of Zn^{2+} binding to *Hp*UreE is very similar to that of Ni^{2+}.[34] Despite this similarity, the interaction of Ni^{2+} and Zn^{2+} with *Hp*UreE occurs with two different binding modes, suggesting that functional metal ion selection can be performed in vivo through different ligand environments and protein conformations.

UreG is a partner of UreE in the urease maturation process: in the presence of *Ka*UreE, the amount of GTP required for the optimal in vitro activation of KAU is reduced,[39] and a direct interaction between *Hp*UreE and *Hp*UreG has been detected both in vivo[40,41] and in vitro.[34] The UreE-UreG protein complex contains two monomers of *Hp*UreG dimerized onto one *Hp*UreE dimer.[34] This interaction is stabilized by the presence of Zn^{2+} ions, and not by the presence of Ni^{2+} ions,[34] suggesting a role for Zn^{2+} in promoting the UreE interaction network. A structural model of this interaction (Figure 8) showed the formation of a new metal binding site at the interface of the dimer of dimers and composed by the residues of *Hp*UreE and *Hp*UreG that are involved in metal binding of each single protein. Consistently, the formation of a novel high affinity Zn^{2+} binding site in the protein complex was observed.[34] These data suggest that both Ni^{2+} and Zn^{2+} are functional in the urease activation process, and that an exchange of these metal ions could modulate the protein interaction network leading to urease maturation. These considerations highlight the reciprocal influence that balanced intracellular levels of different metal ions, such as Ni^{2+} and Zn^{2+}, exert for the correct control of essential biological functions.

Recently, the cross talk among proteins belonging to separated metabolic pathways, but sharing the common motif of activation of nickel-dependent enzymatic systems, has emerged in intracellular nickel trafficking. An example is the interaction between HypA, a Ni^{2+}-binding protein required for the full activity of both [Ni,Fe]-hydrogenase and urease in *H. pylori*,[42] with *Hp*UreE, proposed to allow Ni^{2+} transfer from HypA eventually to apo-urease in *H. pylori*.[43]

The dissection of these intersected pathways, and the understanding of the role of different proteins and metal ions in directing the traffic at these intersections, represents future challenges for the bioinorganic chemistry community.

Supporting Information. Tables SI1 and SI2 reporting, respectively, the classification of complete and incomplete urease operons. This material is available free of charge via the Internet at http://pubs.acs.org.

BIOGRAPHICAL INFORMATION

Barbara Zambelli received a Ph.D. degree in Biotechnology from the University of Bologna in 2006. She was a visiting scientist in 2003 at the University of Gent (Belgium) and in 2005 at EMBL Hamburg (Germany) and has been a Research Associate at the University of Bologna since 2008. Her research is focused on intracellular nickel trafficking.

Francesco Musiani received a Ph.D. degree in Chemistry from the University of Florence in 2003. He is currently a postdoctoral research fellow in the Department of Agro-Environmental Science and Technology at the University of Bologna. His research is focused on biocomputing approaches applied to bioinorganic chemistry.

Stefano Benini received a Ph.D. degree in Chemistry from York University (U.K.) in 2001 with Prof. Keith S. Wilson for his research carried out at the EMBL Hamburg (Germany). He was a Postdoctoral Fellow at the ICGEB Trieste (Italy), University of York, and AstraZeneca (U.K.). He has been a Research Associate at the Free University of Bolzano since 2009. His research is focused on the structural biology of bacterial pathogens.

Stefano Ciurli received a Ph.D. degree in Chemistry from Harvard University (U.S.) in 1990 with Prof. Richard H. Holm. Following postdoctoral studies with Prof. Ivano Bertini (Florence, Italy), he became Associate Professor in 1992 and then Full Professor of Chemistry in 2001 at the University of Bologna. His research is focused on the chemistry of metal ions in biological systems, with special attention to nickel, iron, copper, and zinc.

FOOTNOTES

*To whom correspondence should be addressed. Mailing address: Viale Giuseppe Fanin 40, I-40127 Bologna, Italy. Telephone: +39-051-209-6204. Fax: +39-051-209-6203. E-mail: stefano.ciurli@unibo.it.

REFERENCES

1 Jabri, E.; Carr, M. B.; Hausinger, R. P.; Karplus, P. A. The crystal structure of urease from Klebsiella aerogenes. *Science* **1995**, *268*, 998–1004.

2 Benini, S.; Rypniewski, W. R.; Wilson, K. S.; Miletti, S.; Ciurli, S.; Mangani, S. A new proposal for urease mechanism based on the crystal structures of the native and inhibited enzyme from Bacillus pasteurii: why urea hydrolysis costs two nickels. *Struct. Folding Des.* **1999**, *7*, 205–216.

3 Ha, N.-C.; Oh, S.-T.; Sung, J. Y.; Cha, K. A.; Lee, M. H.; Oh, B.-H. Supramolecular assembly and acid resistance of Helicobacter pylori urease. *Nat. Struct. Biol.* **2001**, *8*, 505–509.

4 Balasubramanian, A.; Ponnuraj, K. Crystal structure of the first plant urease from jack bean: 83 years of journey from its first crystal to molecular structure. *J. Mol. Biol.* **2010**, *400*, 274–283.

5 Callahan, B. P.; Yuan, Y.; Wolfenden, R. The burden borne by urease. *J. Am. Chem. Soc.* **2005**, *127*, 10828-9.

6 Ciurli, S.; Benini, S.; Rypniewski, W. R.; Wilson, K. S.; Miletti, S.; Mangani, S. Structural properties of the nickel ions in urease: novel insights into the catalytic and inhibition mechanisms. *Coord. Chem. Rev.* **1999**, *190−192*, 331–355.

7 Musiani, F.; Arnofi, E.; Casadio, R.; Ciurli, S. Structure-based computational study of the catalytic and inhibition mechanisms of urease. *J. Biol. Inorg. Chem.* **2001**, *6*, 300–314.

8 Benini, S.; Rypniewski, W. R.; Wilson, K. S.; Mangani, S.; Ciurli, S. Molecular details of urease inhibition by boric acid: insights into the catalytic mechanism. *J. Am. Chem. Soc.* **2004**, *126*, 3714–3715.

9 Dixon, N. E.; Gazzola, C.; Blakeley, R.; Zerner, B. Jack bean urease (EC 3.5.1.5). A metalloenzyme. A simple biological role for nickel? *J. Am. Chem. Soc.* **1975**, *97*, 4131–4132.

10 Stoof, J.; Breijer, S.; Pot, R. G.; van der Neut, D.; Kuipers, E. J.; Kusters, J. G.; van Vliet, A. H. Inverse nickel-responsive regulation of two urease enzymes in the gastric pathogen Helicobacter mustelae. *Environ. Microbiol.* **2008**, *10*, 2586–2597.

11 Benanti, E. L.; Chivers, P. T. An intact urease assembly pathway is required to compete with NikR for nickel ions in Helicobacter pylori. *J. Bacteriol.* **2009**, *191*, 2405–2408.

12 Li, Y.; Zamble, D. B. Nickel homeostasis and nickel regulation: an overview. *Chem. Rev.* **2009**, *109*, 4617–4643.

13 Zambelli, B.; Bellucci, M.; Danielli, A.; Scarlato, V.; Ciurli, S. The Ni^{2+} binding properties of Helicobacter pylori NikR. *Chem. Commun.* **2007**, 3649–3651.

14 Dian, C.; Schauer, K.; Kapp, U.; McSweeney, S. M.; Labigne, A.; Terradot, L. Structural basis of the nickel response in Helicobacter pylori: crystal structures of HpNikR in apo and nickel-bound states. *J. Mol. Biol.* **2006**, *361*, 715–730.

15 West, A. L.; St John, F.; Lopes, P. E.; MacKerell, A. D., Jr.; Pozharski, E.; Michel, S. L. Holo-Ni(II) HpNikR is an asymmetric tetramer containing two different nickel-binding sites. *J. Am. Chem. Soc.* **2010**, *132*, 14447–14456.

16 Zambelli, B.; Danielli, A.; Romagnoli, S.; Neyroz, P.; Ciurli, S.; Scarlato, V. High-affinity Ni^{2+} binding selectively promotes binding of Helicobacter pylori NikR to its target urease promoter. *J. Mol. Biol.* **2008**, *383*, 1129–1143.

17 Finney, L. A.; O'Halloran, T. V. Transition metal speciation in the cell: insights from the chemistry of metal ion receptors. *Science* **2003**, *300*, 931–936.

18 Musiani, F.; Bertosa, B.; Magistrato, A.; Zambelli, B.; Turano, P.; Losasso, V.; Micheletti, C.; Ciurli, S.; Carloni, P. Computational Study of the DNA-Binding Protein Helicobacter pylori NikR: The Role of Ni^{2+}. *J. Chem. Theory Comput.* **2010**, *6*, 3503–3515.

19 Kim, J. K.; Mulrooney, S. B.; Hausinger, R. P. Biosynthesis of active Bacillus subtilis urease in the absence of known urease accessory proteins. *J. Bacteriol.* **2005**, *187*, 7150–7154.

20 Carter, E. L.; Flugga, N.; Boer, J. L.; Mulrooney, S. B.; Hausinger, R. P. Interplay of metal ions and urease. *Metallomics* **2009**, *1*, 207–221.

21 Carter, E. L.; Hausinger, R. P. Characterization of the Klebsiella aerogenes urease accessory protein UreD in fusion with the maltose binding protein. *J. Bacteriol.* **2010 192, 22942304.**

22 Chang, Z.; Kuchar, J.; Hausinger, R. P. Chemical cross-linking and mass spectrometric identification of sites of interaction for UreD, UreF, and urease. *J. Biol. Chem.* **2004**, *279*, 15305–15313.

23 Salomone-Stagni, M.; Zambelli, B.; Musiani, F.; Ciurli, S. A model-based proposal for the role of UreF as a GTPase-activating protein in the urease active site biosynthesis. *Proteins* **2007**, *68*, 749–761.

24 Soriano, A.; Hausinger, R. P. GTP-dependent activation of urease apoprotein in complex with the UreD, UreF, and UreG accessory proteins. *Proc. Natl. Acad. Sci. U.S.A.* **1999**, *96*, 11140–11144.

25 Lam, R.; Romanov, V.; Johns, K.; Battaile, K. P.; Wu-Brown, J.; Guthrie, J. L.; Hausinger, R. P.; Pai, E. F.; Chirgadze, N. Y. Crystal structure of a truncated urease accessory protein UreF from Helicobacter pylori. *Proteins* **2010**, *78*, 2839–2848.

26 Moncrief, M. B.; Hausinger, R. P. Characterization of UreG, identification of a UreD-UreF-UreG complex, and evidence suggesting that a nucleotide-binding site in UreG is required for in vivo metallocenter assembly of Klebsiella aerogenes urease. *J. Bacteriol.* **1997**, *179*, 4081–4086.

27 Zambelli, B.; Stola, M.; Musiani, F.; De Vriendt, K.; Samyn, B.; Devreese, B.; Van Beeumen, J.; Turano, P.; Dikiy, A.; Bryant, D. A.; Ciurli, S. UreG, a chaperone in the urease assembly

process, is an intrinsically unstructured GTPase that specifically binds Zn^{2+}. *J. Biol. Chem.* **2005**, *280*, 4684–4695.

28 Zambelli, B.; Musiani, F.; Savini, M.; Tucker, P.; Ciurli, S. Biochemical studies on Mycobacterium tuberculosis UreG and comparative modeling reveal structural and functional conservation among the bacterial UreG family. *Biochemistry* **2007**, *46*, 3171–3182.

29 Zambelli, B.; Turano, P.; Musiani, F.; Neyroz, P.; Ciurli, S. Zn^{2+}-linked dimerization of UreG from Helicobacter pylori, a chaperone involved in nickel trafficking and urease activation. *Proteins* **2009**, *74*, 222–239.

30 Neyroz, P.; Zambelli, B.; Ciurli, S. Intrinsically disordered structure of Bacillus pasteurii UreG as revealed by steady-state and time-resolved fluorescence spectroscopy. *Biochemistry* **2006**, *45*, 8918–8930.

31 Boer, J. L.; Quiroz-Valenzuela, S.; Anderson, K. L.; Hausinger, R. P. Mutagenesis of Klebsiella aerogenes UreG to probe nickel binding and interactions with other urease-related proteins. *Biochemistry* **2010**, *49*, 5859–5869.

32 Musiani, F.; Zambelli, B.; Stola, M.; Ciurli, S. Nickel trafficking: insights into the fold and function of UreE, a urease metallochaperone. *J. Inorg. Biochem.* **2004**, *98*, 803–813.

33 Stola, M.; Musiani, F.; Mangani, S.; Turano, P.; Safarov, N.; Zambelli, B.; Ciurli, S. The nickel site of Bacillus pasteurii UreE, a urease metallo-chaperone, as revealed by metal-binding studies and X-ray absorption spectroscopy. *Biochemistry* **2006**, *45*, 6495–6509.

34 Bellucci, M.; Zambelli, B.; Musiani, F.; Turano, P.; Ciurli, S. Helicobacter pylori UreE, a urease accessory protein: specific Ni(2+)- and Zn(2+)-binding properties and interaction with its cognate UreG. *Biochem. J.* **2009**, *422*, 91–100.

35 Shi, R.; Munger, C.; Asinas, A.; Benoit, S. L.; Miller, E.; Matte, A.; Maier, R. J.; Cygler, M. Crystal structures of apo and metal-bound forms of the UreE protein from Helicobacter pylori: role of multiple metal binding sites. *Biochemistry* **2010**, *49*, 7080–7088.

36 Grossoehme, N. E.; Mulrooney, S. B.; Hausinger, R. P.; Wilcox, D. E. Thermodynamics of Ni^{2+}, Cu^{2+}, and Zn^{2+} binding to the urease metallochaperone UreE. *Biochemistry* **2007**, *46*, 10506–10516.

37 Benoit, S.; Maier, R. J. Dependence of Helicobacter pylori urease activity on the nickel-sequestering ability of the UreE accessory protein. *J. Bacteriol.* **2003**, *185*, 4787–4795.

38 Remaut, H.; Safarov, N.; Ciurli, S.; Van Beeumen, J. J. Structural basis for Ni transport and assembly of the urease active site by the metallo-chaperone UreE from Bacillus pasteurii. *J. Biol. Chem.* **2001**, *276*, 49365–49370.

39 Soriano, A.; Colpas, G. J.; Hausinger, R. P. UreE stimulation of GTP-dependent urease activation in the UreD-UreF-UreG-urease apoprotein complex. *Biochemistry* **2000**, *39*, 12435–12440.

40 Voland, P.; Weeks, D. L.; Marcus, E. A.; Prinz, C.; Sachs, G.; Scott, D. Interactions among the seven Helicobacter pylori proteins encoded by the urease gene cluster. *Am. J. Physiol.* **2003**, *284*, G96–G106.

41 Stingl, K.; Schauer, K.; Ecobichon, C.; Labigne, A.; Lenormand, P.; Rousselle, J. C.; Namane, A.; de Reuse, H. In vivo interactome of Helicobacter pylori urease revealed by tandem affinity purification. *Mol. Cell. Proteomics* **2008**, *7*, 2429–2441.

42 Benoit, S. L.; Mehta, N.; Weinberg, M. V.; Maier, C.; Maier, R. J. Interaction between the Helicobacter pylori accessory proteins HypA and UreE is needed for urease maturation. *Microbiology* **2007**, *153*, 1474–1482.

43 Olson, J. W.; Mehta, N. S.; Maier, R. J. Requirement of nickel metabolism proteins HypA and HypB for full activity of both hydrogenase and urease in Helicobacter pylori. *Mol. Microbiol.* **2001**, *39*, 176–182.